Incorporation of Zwitterionic Push−Pull Chromophores into Hybrid Organic−Inorganic Matrixes

Plinio Innocenzi,* Enrico Miorin, and Giovanna Brusatin

Department of Mechanical Engineering, Materials Section, University of Padova, via Marzolo 9, I-35131 Padova, Italy

Alessandro Abbotto, Luca Beverina, and Giorgio A. Pagani

Department of Materials Science and INSTM, University of Milano-Bicocca, via Cozzi 53, I-20125 Milano, Italy

Mauro Casalboni and Felice Sarcinelli

Department of Physics and INFM, Università di Roma "Tor Vergata", via della Ricerca Scientifica 1, I-00133 Rome, Italy

Roberto Pizzoferrato

Department of Mechanical Engineering and INFM, Università di Roma "Tor Vergata", via di Tor Vergata 110, I-00133 Rome, Italy

Received September 3, 2001. Revised Manuscript Received May 13, 2002

Dihydroxy-functionalized zwitterionic push−pull chromophores have been synthesized and incorporated into 3-glycidoxypropyltrimethoxysilane- and *N*-[(3-trimethoxysilyl)propyl]-ethylenediamine-derived hybrid materials. The functionalization allowed the dye to form covalent bonds to the matrix network, reaching up to 5% molar concentration without aggregation. The host hybrid material was also specifically designed to reduce photobleaching of the dye and to avoid the protonation of the carbanionic species that occurs in acidic media. The host material exhibits very good film-forming properties, and thick highly transparent doped layers can be fabricated via dip-coating. Upon incorporation into the matrix, the dye exhibits a reduction of photobleaching due to the scavenger effect of the amine groups. The strong negative solvatochromism exhibited by this class of chromophores was used to probe the physical-chemical environment within the pores. Dye-functionalized hybrid sol−gel materials were submitted to poling experiments, and the second harmonic signal was measured. Good temporal stability of the NLO materials (retention of ca. 85% of the initial signal value) was recorded after 3 months, providing a d_{33} value equal to 0.66 pm/V. This system represents one of the few examples of the successful incorporation of zwitterionic push−pull chromophores in sol−gel materials.

1. Introduction

Organic second-order nonlinear optical (NLO) materials are the focus of growing interest because of their potential application in signal-processing and telecommunication technologies.[1,2] The design and synthesis of second-order NLO chromophores with large hyperpolarizabilities is the starting point in the development of efficient solid-state NLO devices.[3] Organic polymers and hybrid organic−inorganic materials are two possible candidates for use as host matrixes for NLO chromophores. In particular, several examples of the application of hybrid materials in poling processes with NLO molecules have recently appeared in the literature.[2,4]

Different types of hybrid NLO chromophore materials have been prepared. One group is composed of guest−host systems;[5] however, the maximum chromophore loading for these materials seems limited to about 15−20%, and the NLO response after poling becomes largely unstable with time. A larger group includes systems with covalent bonding between the chromophores and the hybrid network:[6] both side-chain tethered or main-

* Corresponding author.

(1) Wise, D. L.; Wnek, G. E.; Trantolo, D. J.; Cooper, T. M.; Gresse, J. D. *Photonic Polymer Systems*; Marcel Dekker: New York, 1998.

(2) (a) Leigh, W. B. *Devices of Optoelectronics*; Marcel Dekker: New York, 1996. (b) Banach, M. J.; Alexander, M. D., Jr.; Caracci, S.; Vaia, R. A. *Chem. Mater.* **1999**, *11*, 2554.

(3) Zhang, C.; Ren, A. S.; Wang, F.; Zhu, J.; Dalton, L. R. *Chem. Mater.* **1999**, *11*, 1966.

(4) Chaumel, F.; Jiang, H.; Kakkar, A. *Chem. Mater.* **2001**, *13*, 3389.

(5) (a) Zhang, Y.; Prasad, P. N.; Burzynski, R. *Chem. Mater.* **1992**, *4*, 851. (b) Nosaka, Y.; Tohriwa, N.; Kobayashi, T.; Fuji, N. *Chem. Mater.* **1993**, *5*, 930. (c) Zhanjia, J. H.; Liying, Y. L.; Xu, L.; Zhiling, L. X.; Wencheng, C. W.; Li, F. M.; Mingxin, X. L. *Chem. Mater.* **1999**, *11*, 3177.

(6) (a) Sung, P. H.; Hsu, T. F. *Polymer* **1998**, *39*, 1453. (b) Kim, H. K.; Kang, S. J.; Choi, S. K. *Chem. Mater.* **1999**, *11*, 779. (c) Lee, K. S.; Kim, T. D.; Min, Y. H.; Yoon, C. S. *Synth. Met.* **2001**, *117*, 311.

10.1021/cm011231n CCC: $22.00
Published on Web 08/06/2002

chain embedded bonding have been reported. The dyes employed are generally functionalized or modified Disperse Red-type molecules, with similar NLO activities. Functionalization is performed with the main purpose of increasing the poling feasibility and the temporal stability by adjusting the number of anchor points on the hybrid network. A better efficiency, with enhancement of the elecrooptic coefficient, is achieved through the optimization of the chromophore environment.[7]

Compared to the previous works, however, we have decided to use a different family of molecules, with a different perspective. If systems are developed starting with chromophores with very much larger hyperpolarizability values, at least according to NLO measurements of the chromophores in solution, it is reasonable to expect an overall increase of the NLO performances of the final materials. Some of us have recently synthesized a new class of heterocycle-based push−pull chromophores with very large first molecular hyperpolarizabilities ($\beta\mu$ at 1.9 μm as large as 27 000 $\times$ 10^{-48} esu).[8,9] In polar solvents, these dyes exhibit an aromatic and highly zwitterionic ground state and a quinoidal excited state; this is the reverse of the chromophores that are generally used for second-order NLO purposes, which have aromatic and neutral ground states.

The incorporation of zwitterionic dyes into a suitable matrix to fabricate a solid-state device represents, however, quite a challenging task because these dyes show a tendency to photodegrade under the combined action of oxygen and light[10] and because they are sensitive to acidic environments. The matrix, on the other hand, must also fulfill several requirements, such as allowing incorporation of the doping molecules in large amounts while avoiding aggregation effects. The host material should be processed as films having thicknesses of several microns that have low optical propagation losses and are dense at temperatures low enough to avoid thermal degradation of the chromophores.[11] The host material, at the same time, must allow for the orientation of the dyes under poling conditions, to ensure good temporal stability, and must be able to resist intense electrical fields.

We have selected hybrid materials because, in our specific case, they give a larger degree of flexibility[12] in designing the properties of the final material because of the zwitterionic nature of the chromophore and its very specific requirements upon incorporation into a solid matrix. We followed a strategy that links the design of the matrix to that of the guest molecules. The zwitterionic chromophores have been functionalized to enhance their solubility in the polar solvents used in sol−gel film processing and to be covalently bonded to the inorganic side of the network.

Another important aspect that must be carefully evaluated is the matrix−chromophore interaction. Many of the properties of the final material will depend, in fact, on the chemical-physical shell that surrounds the chromophore. A clear understanding of this behavior is very crucial in the development of materials with controlled and temporally stable properties. Indeed, the NLO properties of the materials must be stable for very long times to be useful for practical applications. On the other hand, a low temperature of processing, usually lower than 80 °C, does not allow for full evaporation of the residual solvent (such as water and alcohol) within the pores when hybrid materials are employed as hosts for second-order NLO molecules. This is a parameter that must be carefully evaluated.

The purpose of the present work was to synthesize a hybrid organic−inorganic material that can successfully entrap zwitterionic chromophores. We have designed the sol−gel material to enhance the stability of the optically active molecule upon incorporation into the matrix and to control the chromophore−host material interactions. We have also tested the poling feasibility of the material for future applications in nonlinear optical systems.

2. Experimental Section

2.1. Materials. Tetraethyl orthosilicate (TEOS), 3-(triethoxysilyl)propylamine (TESPA), 3-glycidoxypropyltrimethoxysilane (GPTMS), and *N*-[(3-trimethoxysilyl)propyl]ethylenediamine (TMESPE) were purchased from Aldrich and employed without further purification. Methyl alcohol (MeOH) (Prolabo) was used as the solvent, and bidistilled water was used for hydrolysis.

2.2. Synthesis of the Chromophore (Scheme 1). *1-[N-(3-bromopropyl)pyrid-4-yl]-2-[5-(dicyanomethanido)thien-2-yl]-ethylene*, ***3***. A solution of 3-bromopropyl triflate[13] (0.950 g, 3.51 mmol) in dry acetone (5 mL) was added dropwise, under a nitrogen atmosphere, to a solution of 1-(4-pyridyl)-2-[5-(dicyanomethanido)thien-2-yl]ethylene sodium salt[8a] (0.681 g, 2.5 mmol) in the same solvent (5 mL). The reaction mixture was stirred overnight at room temperature. The dark precipitate that formed was filtered off under reduced pressure and washed with ethanol (5 mL), yielding the product as a blue solid (0.475 g, 51%), which was used for the subsequent step without any further purification. mp = 239−240 °C. ^{1}H NMR (DMSO-d_6) δ (ppm): 2.41 (m, 2H), 3.53 (t, J = 6.6 Hz, 2H), 4.36 (t, J = 7.0 Hz, 2H), 6.28 (d, J = 4.1 Hz, 1H), 6.32 (d, J = 15.1 Hz, 1H), 7.21 (d, J = 4.2 Hz, 1H), 7.74 (d, J = 7.0 Hz, 2H), 8.00 (d, J = 15.1 Hz, 1H), 8.43 (d, J = 7.0 Hz, 2H).

1-[N-(3-N′-Diethanolaminopropyl)pyrid-4-yl]-2-[5-(dicyanomethanido)thien-2-yl)ethylene, ***2*** *(BisOH·PETCN).* Powdery brominated precursor **3** (0.200 g, 0.54 mmol) was added, under a nitrogen atmosphere, to a solution of diethanolamine (0.341 g, 3.24 mmol) in anhydrous acetonitrile (10 mL). The reaction mixture was kept under reflux for 4 h and then cooled in an ice bath. A dark precipitate was filtered off and crystallized, under a nitrogen atmosphere, from dry ethanol, yielding the product as a dark-blue solid (0.139 g, 78%). mp = 230 °C.

Anal. Found (calcd.) for $C_{21}H_{24}N_4O_2S\cdot{}^1/_2H_2O$: C 61.98 (62.20), H 6.38 (6.21), N 13.61 (13.82). ^{1}H NMR (DMSO-d_6) δ (ppm): 1.98 (m, 2H), 2.45 (t, J = 6.4 Hz, 2H), 2.49 (t, J = 6.4 Hz, 4H), 3.41 (t, J = 5.4 Hz, 4H), 4.33 (t, J = 6.9 Hz, 2H), 4.41 (s, 2H), 6.26 (d, J = 4.1 Hz, 1H), 6.34 (d, J = 15.1 Hz, 1H),

(7) Banach, M. J.; Alexander, M. D.; Caracci, S.; Vaia, R. A. *Chem. Mater.* **1999**, *11*, 2554.

(8) (a) Abbotto, A.; Bradamante, S.; Facchetti, A.; Pagani, G. A. *J. Org. Chem.* **1997**, *62*, 5755. (b) Abbotto, A.; Bradamante, S.; Facchetti, A.; Pagani, G. A.; Ledoux, I.; Zyss, J. *Mater. Res. Soc. Symp. Proc.* **1998**, *488*, 819.

(9) Abbotto, A.; Bozio, R.; Brusatin, G.; Facchetti, A.; Guglielmi, M.; Innocenzi, P.; Meneghetti, M.; Pagani, G. A.; Signorini, R. *Proc. SPIE* **1999**, *3803*, 18.

(10) Abbotto, A.; Beverina, L.; Bradamante, S.; Facchetti, A.; Pagani, G. A.; Ledoux, I.; Zyss, J. Unpublished results, 2002.

(11) Sanchez, C.; Lebeau, B. *MRS Bull.* **2001**, 377.

(12) (a) Innocenzi, P.; Brusatin, G.; Guglielmi, M.; Bertani, R. *Chem. Mater.* **1999**, *11*, 1672. (b) Innocenzi, P.; Brusatin, G.; Babonneau, F. *Chem. Mater.* **2000**, *12*, 3726. (c) Innocenzi, P.; Sassi, A.; Brusatin, G.; Guglielmi, M.; Favretto, D.; Bertani, R.; Venzo, A.; Babonneau, F. *Chem. Mater.* **2001**, *13*, 3635.

(13) Chi, D. Y.; Kilbourn, M. R.; Katznellenbogen, J. A.; Welch M. J. *J. Org. Chem.* **1987**, *52*, 658.

Scheme 1

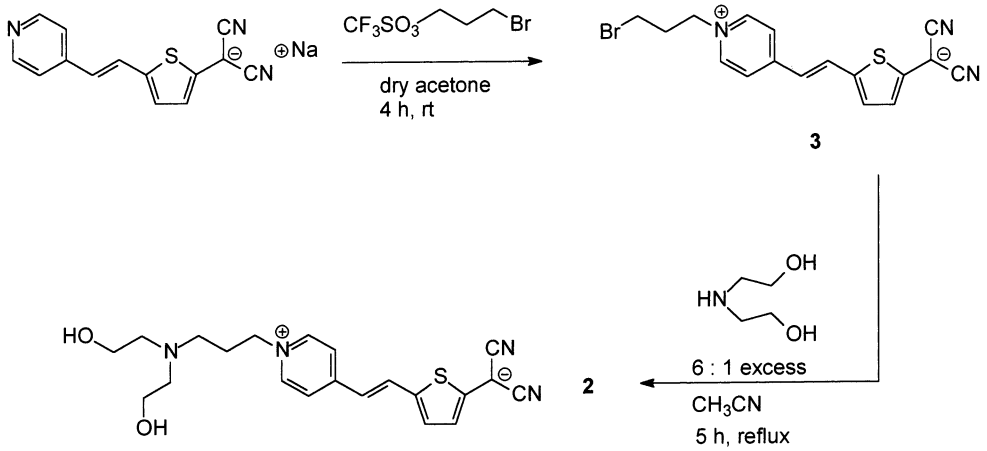

Scheme 2

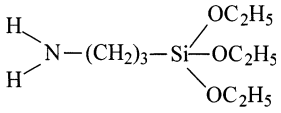

3-(triethoxysilyl)-propylamine (TESPA)

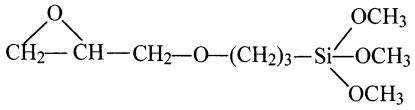

N-[3-(trimethoxy-silyl)propyl]ethylenediamine (TMESPE)

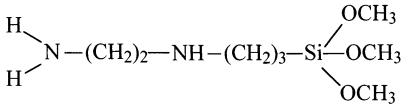

3-glycidoxypropyltrimethoxysilane (GPTMS)

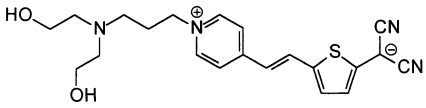

1-[*N*-(diethanolaminopropyl)pyrid-4-yl]-
2-[5-(dicyanomethanido)thien-2-yl]ethylene (BisOH.PETCN)

7.21 (d, $J = 4.2$ Hz, 1H), 7.74 (d, $J = 6.9$ Hz, 2H), 7.99 (d, $J = 15.1$, 1H), 8.46 (d, $J = 6.9$ Hz, 2H).

2.3. 3-Glycidoxypropyltrimethoxysilane−3-(Triethoxysilyl)propylamine (GTE) Matrixes (Scheme 2). 3-(Triethoxysilyl)propylamine (TESPA) was mixed with 3-glycidoxypropyltrimethoxysilane (GPTMS) and methyl alcohol (MeOH). Different TESPA/GPTMS molar ratios were used, ranging from 6.7×10^{-2} to 0.54×10^{-2}. H_2O was added dropwise for the hydrolysis in molar ratios of $H_2O/SiO_2 = 5.3$ and $MeOH/SiO_2 = 1.7$. After addition of the water, the sol was reacted at 60 °C for 30 min. BisOH·PETCN in MEOH was finally added and left to react for 10 min at 25 °C. The relative concentration of BisOH·PETCN in the matrix, with respect to the number of moles of silicon, was 5%.

2.4. 3-Glycidoxypropyltrimethoxysilane−*N*-[(3-Trimethoxysilyl)propyl]ethylenediamine (GTM) Matrixes. A procedure similar to that employed for GTE was used to synthesize the material from *N*-[(3-trimethoxysilyl)propyl]-ethylenediamine (TMESPE) (Scheme 2) and GPTMS. The molar ratios were TMESPE/GPTMS = $6.7-0.54 \times 10^{-2} = 1240$, $MeOH/SiO_2 = 1.7$, and $H_2O/SiO_2 = 5.3$. BisOH·PETCN had a concentration of 5×10^{-3} M.

2.5. 3-Glycidoxypropyltrimethoxysilane−*N*-[(3-Trimethoxysilyl)propyl]ethylenediamine−Tetraethoxysilane (GTMT) Matrixes. A third host material was prepared using GPTMS, TMESPE, and tetraethoxysilane (TEOS). GPTMS was co-hydrolyzed with TEOS and reacted for 1 h under reflux at 80 °C (buffer sol GT). BisOH·PETCN in a saturated solution of MeOH and TMESPE was added immediately afterward to GT, and the mixture was left under magnetic stirring at 25 °C for 10 min. The films were deposited from the freshly prepared sols. The molar ratios employed were GPTMS/TEOS = 7/3, TMESPE/(GPTMS + TEOS) = 0.37−0.94, $H_2O/SiO_2 = 1-8$, and $MeOH/SiO_2 = 10.1-8.47$. The chromophore BisOH·PETCN was added to reach a 5% molar concentration with respect to SiO_2 in the matrix.

2.6. Material Preparation and Characterization. Films were deposited by spin-coating or dip-coating immediately after preparation of the sol. The samples were dried in air at different temperatures in the range 50−300 °C. To measure the gelation time, the precursor sol was left sealed in a beaker until a gel phase was observed.

Absorption spectra of hybrid doped films deposited on silica slides were recorded in the range 190−800 nm at room temperature as a function of time during the duration of the samples in dark or bright environments. A Perkin-Elmer λ-3B spectrophotometer with a resolution ±0.3 nm was used.

Angle-resolved absorption measurements were carried out using polarized light (incidence angle 30°) to verify the chromophore alignment.

A Gaussian peak-fitting procedure was applied to the absorption spectra (Microcal Origin Software). The quality of the fit was evaluated on the base of the χ^2 values, on the order of 10^{-6}.

Infrared absorption spectra in the range 6500−400 cm^{-1} were recorded on a Fourier transform infrared (FTIR) spectrometer (Perkin-Elmer 2000) with a resolution of ±1 cm^{-1} on films deposited on silicon wafers.

2.7. Poling Experiments. Poling was carried out by using the standard setup and procedure for high-voltage corona poling[14] for 220 min at 85 °C. The corona discharge was generated under a nitrogen atmosphere by a gold wire biased with +7000 V across a 1-cm gap normal to the sol−gel film. Second harmonic generation (SHG) measurements were performed during this procedure and afterward at regular time intervals by using a Q-switched Nd:YAG laser, operating at 1.064 μm, as the source of the fundamental wave.

3. Results and Discussion

3.1. Effect of Amine-Functionalized Alkoxides on Film-Forming Ability of GPTMS-Based Hy-

(14) Mortazavi, M. A.; Knoesen, A.; Kowel, S. T.; Higgins, B. G.; Dienes, A. *J. Opt. Soc. Am. B* **1989**, *6*, 733.

Table 1. Films Prepared from GTMT Sols with Different Amounts of Alkoxides, Water, and Solvent

sample	H_2O/SiO_2	GTMT/(GPTMS + TEOS)	CH_3OH/SiO_2	t_g[a] (min)	film appearance[b]
GTMT147		0.47	10.10	n.o.[c]	opaque, with aggregates
GTMT166	1	0.66	8.95	n.o.	opaque, with aggregates
GTMT175		0.75	8.47	n.o.	partially opaque, aggregates
GTMT247		0.47	10.10	80	transparent, no aggregates
GTMT266	2	0.66	8.95	65	highly transparent, no aggregates
GTMT275		0.75	8.47	53	transparent, some aggregates
GTMT347		0.47	10.10	65	transparent, no aggregates
GTMT366	3	0.66	8.95	45	transparent, no aggregates
GTMT375		0.75	8.47	40	transparent, some aggregates
GTMT447		0.47	10.10	40	transparent, some aggregates
GTMT466	4	0.66	8.95	15	partially opaque, aggregates
GTMT475		0.75	8.47	0	partially opaque, aggregates
GTMT637		0.37	10.78	80	transparent, no aggregates
GTMT647	6	0.47	10.10	75	transparent, some aggregates
GTMT666		0.66	8.95	5	−
GTMT837		0.37	10.78	90	transparent, some aggregates
GTMT847	8	0.47	10.10	80	partially opaque, aggregates
GTMT866		0.66	8.95	10	opaque, aggregates

[a] Gelification time (t_g) reported in minutes. [b] Films classified as they appear upon inspection by optical microscopy to detect the presence of aggregates and by UV−vis spectroscopy to check the optical transmittance in the UV−vis range. [c] n.o. = gelification not observed after several days.

brids. The use of organically modified alkoxides containing amine functionalities in sol−gel synthesis of hybrids has a strong effect on the final properties of the material,[15] particularly on the capability of the precursor sol to form transparent and homogeneous films thicker than 1 μm. These requirements represent, in fact, the *minimum* to be satisfied by the material for photonic applications.[16] In particular, it should be considered that TMESPE and TESPA play a double role during synthesis. They act as strong bases that promote the inorganic polymerization and simultaneously catalyze the opening of the epoxy ring in GPTMS. TMESPE and TESPA also have the effect of modifying the network, because the organic group that terminates the amine functionalities will directly bond to the silica backbone and will react by a coupling reaction with the epoxy rings of GPTMS.[17] A limitation in employing large amounts of TESPA or TMESPE in the synthesis of GPTMS-based hybrids is the very rapid increase in the gelation time when large amounts of amine-functionalized alkoxides are employed. This effect, together with uncontrolled phase separation, makes the possibility of obtaining homogeneous and transparent films quite difficult. The gelation times of GTE, GTM, and GTMT as a function of TESPA and TMESPE contents are shown in Figure 1. In general, the films obtained from GTE and GTM sols are partially opaque or form small aggregates. Much better results were achieved with GTMT sols, which were the subject of a systematic investigation. The effects of the water, MeOH, and TMESPE contents were studied with the purpose of obtaining highly transparent and homogeneous films from a sol that is stable in a time range of several hours. The sols tested and their film capabilities are reported in Table 1, together with their gelation times, t_g. The gelation times of these systems range from few seconds to 100 h with low TESPA and TMESPE contents. However, in GTMT samples, the gelation time can be on the order of minutes with much larger amounts of amine functional groups than in the GTE and GTA systems, while at the same time yielding highly transparent films. In particular, GTMT247 and GTMT266 showed a combination of time stability and high optical

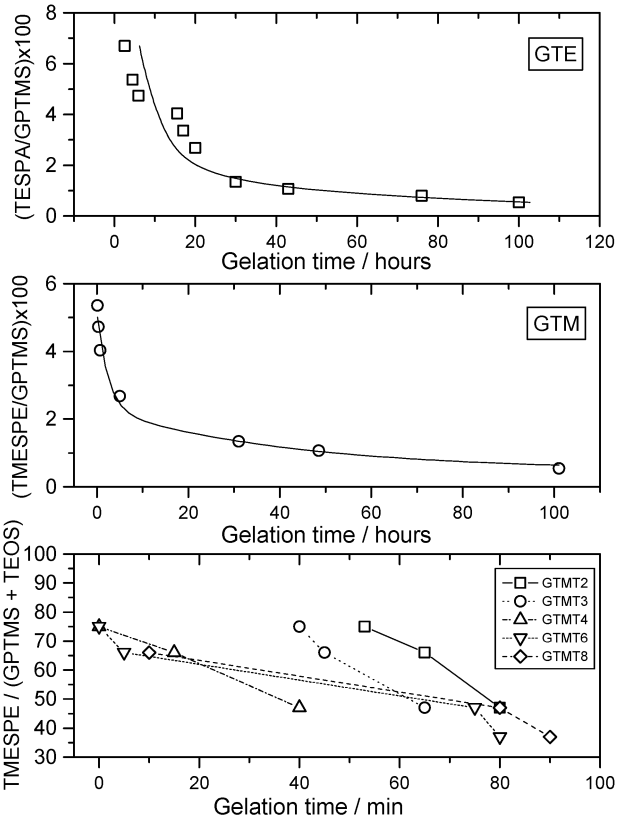

Figure 1. Gelation times of the sols GTE, GTM, and GTMT for different contents of amine-functionalized alkoxides. The lines are guides for the eyes.

(15) Riegel, B.; Blittersorf, S.; Kiefer, W.; Hofacker, S.; Muller, M.; Schottner, G. *J. Non-Cryst. Solids* **1998**, *226*, 76.
(16) (a) Innocenzi, P.; Martucci, A.; Guglielmi, M.; Armelao, L.; Battaglin, G.; Pelli, S.; Righini, G. C. *J. Non-Cryst. Solids* **1999**, *259*, 189. (b) Brusatin, G.; Guglielmi, M.; Innocenzi, P.; Martucci, A.; Battaglin, G.; Pelli, S.; Righini, G. *J. Non-Cryst. Solids* **1997**, *220*, 202.
(17) Brusatin, G.; Guglielmi, M.; Innocenzi, P.; Babonneau, F. *J. Sol−Gel Sci. Technol.* **2002**, in press.

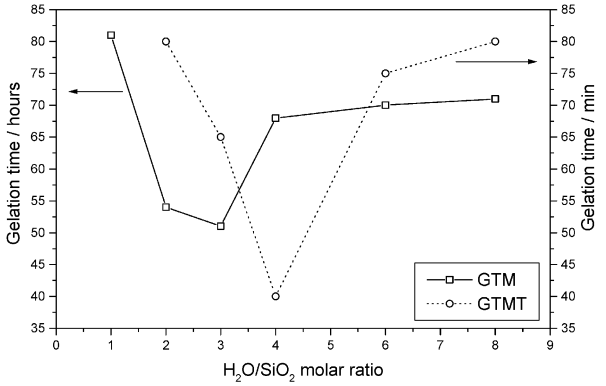

Figure 2. Gelation times of GTM and GTMT sols as a function of water content. The lines are guides for the eyes.

quality and were selected as the best-performing matrixes for BISOH·PETCN. FTIR analysis of GTMT247 and GTMT266 films showed that TMESPE efficiently catalyzed epoxy opening in GPTMS.

The influence of water content on the gelation time is shown in Figure 2 for the GTM and GTMT sols. Even though on different time scales, hours for GTM and minutes for GTMT, the sols exhibit similar trends. The gelation time first decreases with increasing water content and then increases again when a larger amount of water dilutes the sol, similarly to what has been observed in silica sols.[18]

3.2. Photostability of BisOH·PETCN upon Incorporation into Basic-Catalyzed Hybrid Materials. In the Introduction section, it was pointed out that chromophores of the family of BisOH·PETCN are degraded in the presence of light and oxygen.[10] The mechanism of degradation involves singlet oxygen; because of the presence of the intramolecular charge transfer band, the chromophores absorb photons that allow for the excitation of molecular oxygen to singlet oxygen. It has been observed that the presence of amine groups significantly reduces the photobleaching process.[10]

The UV−vis spectra of BisOH·PETCN are characterized by a broad intense absorption band peaking around 630 nm due to intramolecular charge transfer (ICT) (Figure 3). Another band at 380 nm is assigned to electronic transitions within the aromatic rings. A decrease in intensity of the ICT band is associated with degradation of the chromophores.

BisOH·PETCN is completely photobleached within a few days in a protic solvent. Observations of the changes in the absorption spectra of the chromophore in GTMT247 sols under dark and bright conditions show that, in dark environments, the ICT absorption band remains basically stable, showing that the basic environment in the sol avoids the chemical degradation that occurs in acidic media through the protonation of the carbanionic site of the donor moiety. The stability of the molecule is also very largely enhanced upon light exposure, and even though photobleaching cannot be completely avoided, high optical activity is still observed after several months.

Upon incorporation into GTE and GTM matrixes, where much smaller numbers of amine groups can be present in the network to shield the chromophore from singlet oxygen, complete degradation of the chromophore is observed after 30 h under bright conditions and after 60 h in the dark. A dramatic increase in protection from photobleaching is reached upon introduction of the chromophore into GTMT247 matrixes (Figure 3). In dark environments, the material is stable for several months, whereas under bright conditions, the resistance to photobleaching is also remarkably enhanced, as can be appreciated by comparing the change of the absorbance intensity with time in BisOH·PETCN-doped GTM and GTMT samples (Figure 4).

Upon incorporation of BisOH·PETCN into the hybrid materials, a change in the ICT absorption band is observed. A shoulder around 580 nm, attributed to a dimeric form of BisOH·PETCN, is detected in the as-

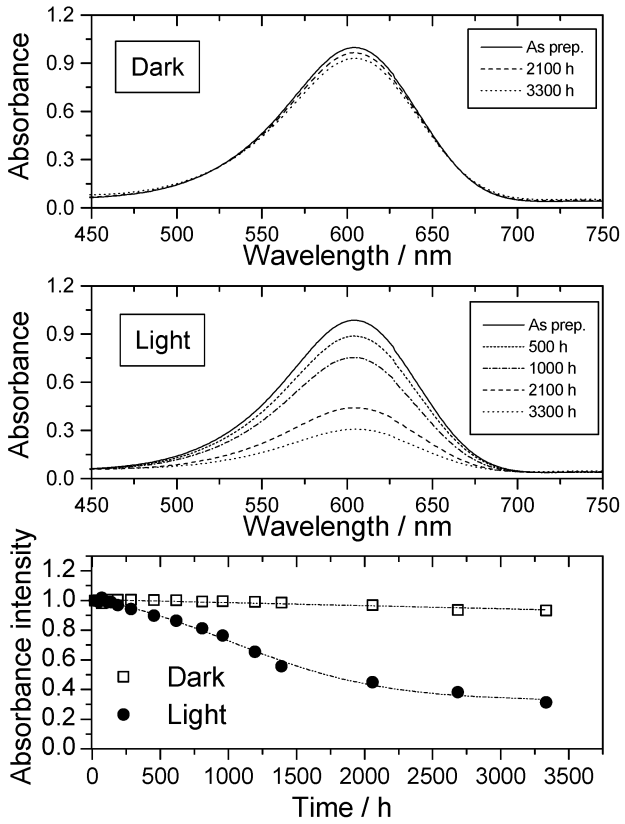

Figure 3. UV−vis absorption spectra of BisOH·PETCN after incorporation into GTMT247 matrixes maintained at 25 °C under dark (top) and bright (bottom) conditions.

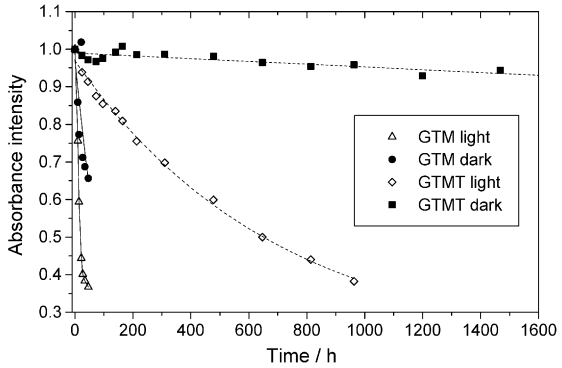

Figure 4. Time dependence of the UV−vis absorbance (normalized values at $\lambda = 630$ nm) of BisOH·PETCN after incorporation into GTM and GTMT247 matrixes.

(18) Brinker, C. J.; Scherer, G. *Sol−Gel Science*; Academic Press: New York, 1989.

deposited films.[19] This form of dimer is assumed to be formed via bridging molecules of the residual solvent within the pores, similary to what has been described for the incorporation of rhodamine 6G in sol−gel silica films.[20] During evaporation of the solvent, which is observed with longer times or after thermal treatments, this shoulder disappears (Figure 4), supporting our hypothesis. At 440 nm another absorption band is observed, which, however, we could not unambiguously attribute. At this wavelength, in fact, molecules of this family usually show an intense narrow band due to high-order aggregates of the "deck-of-cards" type.[21] The presence of these aggregates after incorporation into the matrix is, however, difficult to rationalize, as it should appear as a macroscopic defect of the film, which is not observed. Also, the evolution with time of the band suggests an alternative description. Indeed, the band is not observed after deposition but starts to appear after longer times of incorporation into the matrix; it is not detected in the sol either. The absorption band of the carbanion formed from the zwitterionic chromophores is also present at 440 nm. The carbanion could be formed after evaporation of the solvent, when the dye is directly interacting with the Si−OH groups of the pore surface, which, in a basic environment, can transform the molecule into the carbanion.

The thermal stability of BisOH·PETCN upon incorporation into GTMT247 matrixes is shown in Figure 5. The samples were all treated in air for 30 min at different temperatures. At 150 °C, about 20% of the chromophores are degraded, and the absorption band completely disappears at 250 °C.

3.3. Interaction of the Dye with the Environment and Local Probing Effects. Another interesting property of BisOH·PETCN is its solvatochromism,[8a] which is strictly connected to its hyperpolarizability.[22] Figure 6 shows the UV−vis absorption spectra of BisOH·PETCN in some solvents and, for reference, in GTMT sol and after incorporation into the hybrid matrix. The values of λ_{max} are listed in Table 2, together with $\Delta\lambda$ values calculated with respect to THF. The position of the CT absorption band in the visible region shows a strong solvatochromic shift, which, from H_2O to THF, is about 116 nm toward longer wavelengths. The ICT absorption band of the chromophore therefore exhibits a strong negative solvatochromism; that is, the position of the λ_{max} shifts to shorter wavelengths with increasing solvent polarity (Figure 6). A negative solvatochromism is classically interpreted[23] as an indication that the value of the dipole moment is smaller in the excited state than in the ground state. This behavior is therefore due to the transition from the zwitterionic ground state to the less dipolar excited state, and the main absorption band is definitely assigned to charge transfer from the negatively charged dicyanomethanide group to the positively charged pyridinium ring.

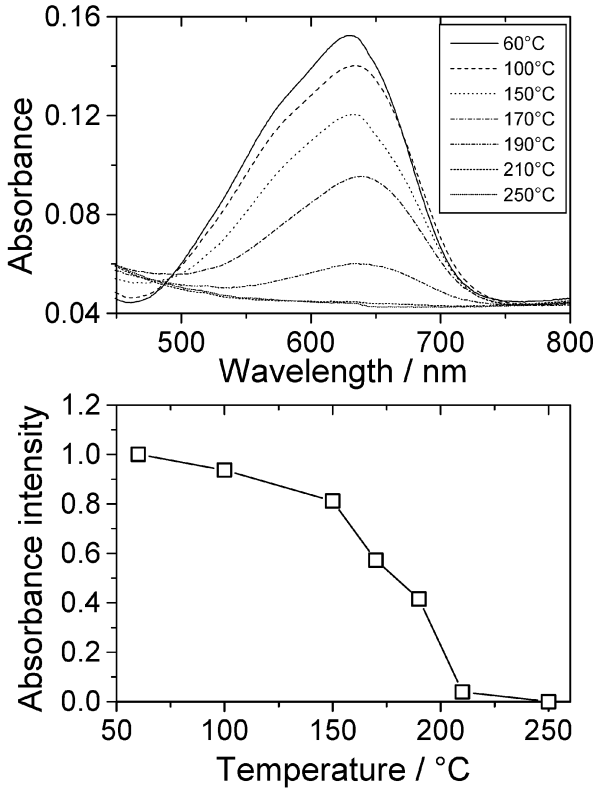

Figure 5. Thermal stability of BisOH·PETCN upon incorporation into GTMT247 matrixes (top) and change in absorbance intensity as a function of thermal treatment temperature (bottom).

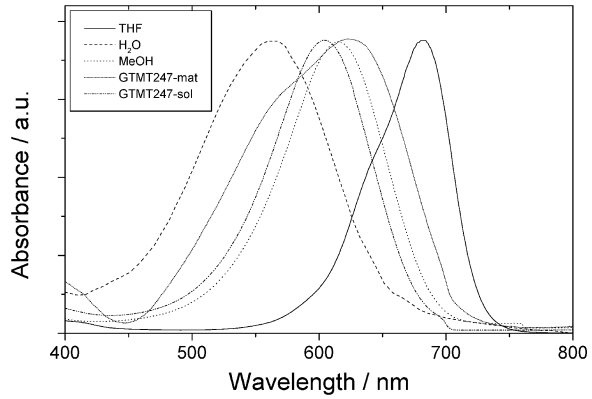

Figure 6. UV−vis absorption spectra of BisOH·PETCN in THF, H_2O, MeOH, GTMT247 sol, and GTMT247 matrix.

Table 2. Solvatochromic Data[a] of BisOH·PETCN in Different Solvents, in the Precursor Sol, and upon Incorporation into the Matrix

solvent	λ_{max} (nm)	$\Delta\lambda^b$
THF	680	−
$GTMT247_{matrix}$	624	−56
methanol	616	−64
$GTMT247_{sol}$	604	−76
H_2O	564	−116

[a] λ_{max} (nm) of the charge transfer band. [b] $\Delta\lambda = \lambda_{max} - \lambda_{max}$ (THF).

Because of its dramatically large solvatochromism, BisOH·PETCN can also be considered a local probe of the changes in the chemical environment after its incorporation into the matrix. Significant shifts of λ_{max}

(19) Mishra, A.; Behera, R. K.; Behera, P. K.; Mishra, B. K.; Behera, G. B. *Chem. Rev.* **2000**, *100*, 1973.
(20) Innocenzi, P.; Kozuka, H.; Yoko, T. *J. Non-Cryst. Solids* **1996**, *201*, 26.
(21) Ricceri, R.; Grando, D.; Abbotto, A.; Facchetti, A.; Pagani, G. A.; Gabrielli, G. *Langmuir* **1997**, *13*, 5787.
(22) (a) Buckeley, A.; Choe, E.; DeMartino, R.; Leslie, T.; Nelson, G.; Starnatoff, J.; Stuetz, D.; Yoon, H. *Polym. Mater. Sci. Eng.* **1986**, *54*, 502. (b) Paley, M. S.; Harris, J. M.; Looser, H.; Baumert, J. C.; Bjorklund, G. C.; Jundt, D.; Twieg, R. J. *J. Org. Chem.* **1989**, *54*, 3774.
(23) Reichardt, C. *Solvents Effects in Organic Chemistry*; Verlag Chemie: New York, 1979; Chapter 6.

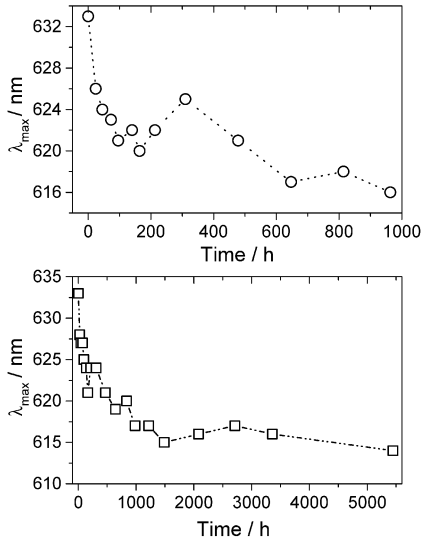

Figure 7. Shift of λ_{max} of BisOH·PETCN in the GTMT247 matrix. The spectra were recorded at different times from samples maintained at room temperature under dark and bright conditions.

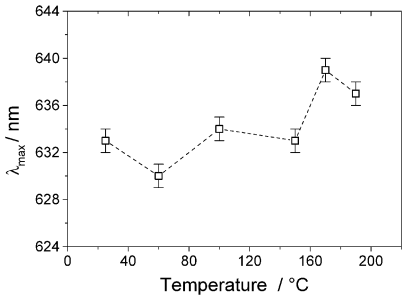

Figure 8. Shift of λ_{max} of BisOH·PETCN in the GTMT247 matrix as a function of drying temperature.

of the ICT band are, in fact, observed with time and after thermal treatment. Figure 7 shows the shift of λ_{max} of BisOH·PETCN in the GTMT247 matrix. The spectra were recorded at different times from samples maintained at room temperature under either dark or bright conditions. A shift to lower wavelengths for times up to around 1000 h is clearly observed in both the samples. The photobleached sample, however, exhibits quite different behavior, as its λ_{max} first decreases, then increases at 400 h, and finally decreases again. This difference is likely due to different photobleaching behaviors of the aggregate species, such as the dimers, clearly observed in the as-deposited samples, with respect to the monomeric form of the chromophore. Shifts of λ_{max} were also clearly observed upon thermal treatment (Figure 8). In this case, the absorption maximum was shifted toward lower wavelengths, from the as-deposited (25 °C) samples to the samples dreid at 60 °C, and is shifted to longer wavelengths at higher drying temperatures. It should be mentioned that, even though solvatochromic dyes have been widely used to probe changes in the local environment within sol−gel materials,[24] BisOH·PETCN shows one of the largest effects among the dyes reported in the literature. The absorption shifts as a function of temperature and time point toward a model that indicates the nature of the chemical environment around the dye molecules and its changes, upon entrapment in the hybrid matrix, with time and temperature. First, an effect due to the evaporation of alcohol, specifically, the residual methanol from the sol that is still entrapped within the pores after film deposition, is present. As the solvent slowly escapes from the pores of the samples maintained at room temperature, an increase in the polarity in the chemical shell around the chromophores occurs. Water is the other residual molecule from the sol−gel reaction that remains within the pores. The chromophores, therefore, are initially solvated by a first chemical shell composed of methanol, which, after its evaporation, is replaced by a second shell formed of residual water. This change is reflected in the increased polarity of the chemical environment. A similar behavior was previously observed upon the incorporation of tris(2,2′-bipyridyl)ruthenium(II) complexes in silica films.[25] This model is supported by the shifts in λ_{max} observed during different thermal treatments. At the first drying stage (25−60 °C), evaporation of residual alcohol is the main mechanism. The polarity around the chromophores increases as the chemical shell is again formed by residual water molecules (Figure 9). At temperatures higher than 100 °C, when water evaporates as well, the polarity decreases as a consequence of the direct interaction of the chromophores with the less polar pore surfaces.

3.4. Poling of the System. The AGT47-doped films were submitted to a poling process at 85 °C. Figure 10a and b shows the second harmonic (SH) signal and the poling temperature, respectively, during the poling process. The orientation efficiency grows during the process and, a stable signal is observed after 2 h. A slight decrease is detected when the temperature is decreased below 40 °C. After poling off, the SHG signal immediately breaks down at a lower but stable value, as has been found in similar sol−gel materials. Undoped hybrid matrixes do not exhibit any SHG signal. No surface degradation was observed during the poling experiments, a particularly important observation in view of the potential waveguide applications of these materials. Moreover, the GTMT247 system exhibits good temporal stability, as confirmed by the SH signal, which remains at about 85% of the initial signal after 3 months. These results confirm the potentially high performances of these new hybrid matrixes as hosts for NLO chromophores.

The order parameter, Φ, was estimated by using the d_{33} measurement after poling off as an efficiency reference value of SHG and making angle-resolved absorption measurements before and after film poling (Figure 3).[26,27] The absorption spectra show a bathochromic shift after poling that can be attributed to large electrostatic fields created by the charges deposited during the poling procedure, which are expected to disappear in few hours. In fact, absorption measurements performed 1 day after poling showed the recovery of the initial absorption peak wavelength, thus confirming this explanation.

(24) Zink, J. I.; Dunn, B. In *Sol−Gel Optics: Processing and Applications*; Klein, L. C., Ed.; Kluwer Academic Publishers: Boston, 1994; p 303.

(25) Innocenzi, P.; Kozuka, H.; Yoko, T. *J. Phys. Chem. B* **1997**, *101*, 2285.

(26) Graf, H. M.; Zobel, O.; East, A. J.; Haarer, D. *J. Appl. Phys.* **1994**, *75*, 3335.

(27) Cao, X.; McHale, J. L. *J. Phys. Chem. B* **1997**, *101*, 8843.

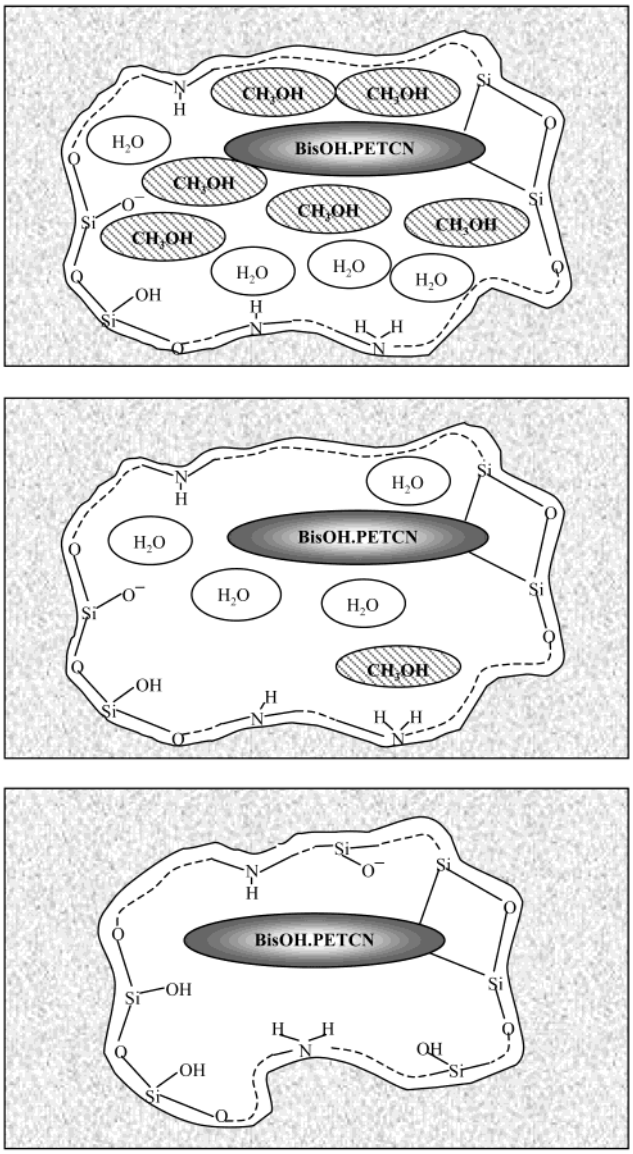

Figure 9. Model of the local changes in the chemical shell around BisOH·PETCN. Immediately after film deposition, the dye is surrounded by a first chemical shell of residual methanol molecules and by a second shell of residual water molecules (top). Upon alcohol evaporation, during drying, the dye is solvated by residual water molecules (middle). After thermal treatment at temperatures higher than 100 °C (water evaporation), the dye interacts with the pore surface (bottom).

The absorption spectra before and after poling are shown in Figure 11a and b, respectively. The spectra are deconvoluted taking into account the presence of two components, fitted by two Gaussian curves, that are likely due to aggregates (at lower wavelengths) and monomers (at larger wavelengths). The deconvolution shows that the dimeric component is not affected by the poling process and can be considered centrosymmetric, whereas the monomeric component shows a significant decrease in intensity after poling (Figure 11c). We have calculated the order parameter from the monomeric curve and obtained a value of $\Phi = 0.34$, which is quite large compared with the values reported in the literature for poled NLO chromophores in sol−gel systems.

The SH signal of the samples under investigation was compared with the second harmonic intensity generated by a Y-cut quartz crystal via the standard Maker fringes

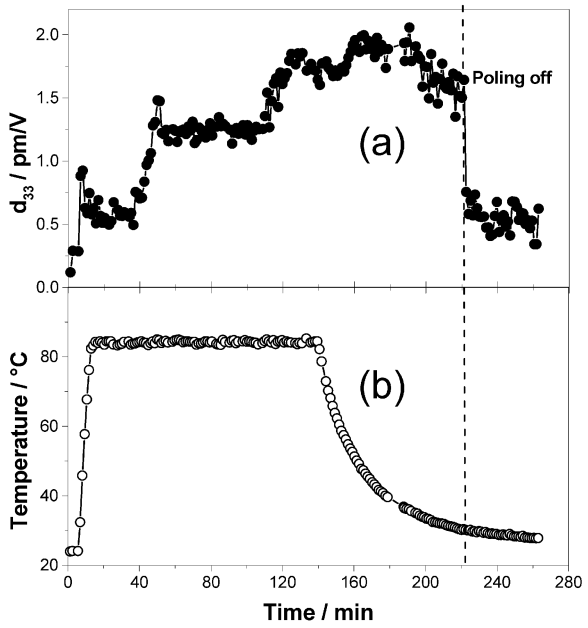

Figure 10. (a) SH signal and (b) poling temperature during the poling process performed at 85 °C on the as-deposited doped films of GTMT247.

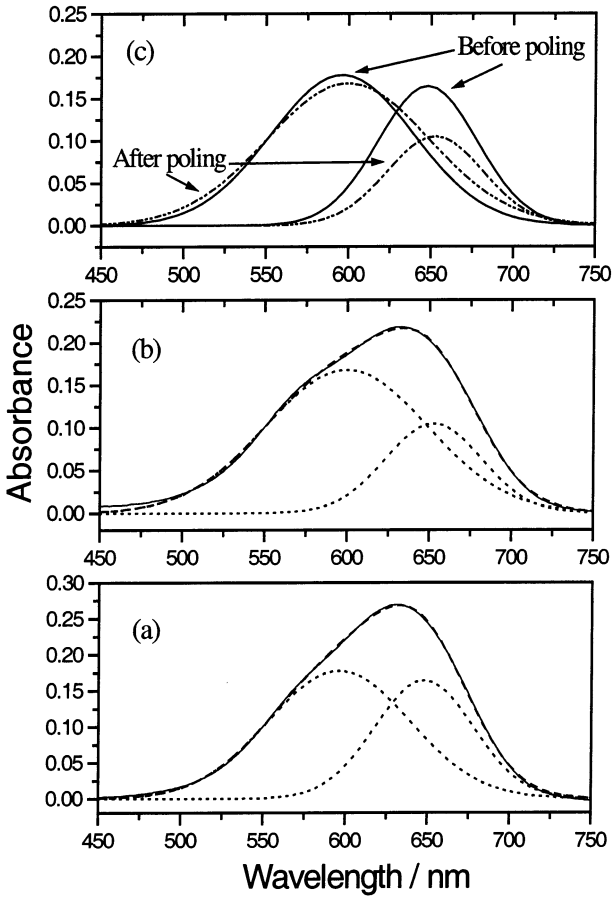

Figure 11. Angle-resolved absorption measurements (a) before and (b) after film poling. The spectra are deconvoluted into two Gaussian components assigned to monomeric and dimeric form of BisOH·PETCN. (c) The deconvoluted bands obtained from the spectra before and after poling are superimposed for comparison.

technique.[28,29] This provides an estimate for the nonlinear coefficient d_{eff} of the samples at a value 2 times

greater than d_{11} of quartz, which, from literature data, is about 0.335 pm/V.[30]

4. Conclusions

Hybrid organic−inorganic materials synthesized under basic conditions from 3-glycidoxypropyltrimethoxysilane and *N*-[(3-trimethoxysilyl)propyl]ethylenediamine) allow for the deposition of highly transparent thick films. A large amount, up to 43 mol %, of amine functionalities were introduced in the matrix. This matrix is suitable for the incorporation of zwitterionic push−pull chromophores functionalized with two hydroxy groups, which allows grafting to the matrix network via covalent bonding. The amine groups were very effective in reducing photobleaching from singlet oxygen. Because of the zwitterionic nature of the dye, a strong solvatochromism effect was observed as a function of the host medium polarity. The solvatochromism was used to probe the local changes with time and temperature in the chemical environment of the molecules within the host matrix. The chromophores are solvated by a first chemical shell composed of residual alcohol molecules immediately after film deposition; a second shell is formed by water molecules, which surround the dye after alcohol evaporation and shield it from direct interactions with the matrix pore surface.

The poling feasibility of this matrix−dye system was demonstrated, without decomposition of the film surface and with good temporal stability.

CM011231N

(28) Jerphagnon, J.; Kurtz, S. K. *J. Appl. Phys.* **1970**, *41*, 1667.
(29) Singer, K. D.; Sohn, J. E.; Lalama, S. J. *Appl. Phys. Lett.* **1986**, *49*, 248.
(30) *CRC Handbook of Chemistry and Physics*, 76th ed.; Lide, D. R., Ed.; CRC Press: Boca raton, FL, 1996.